NASA Technical Memorandum 100279

Structural Dynamics Branch Research and Accomplishments for FY 1987

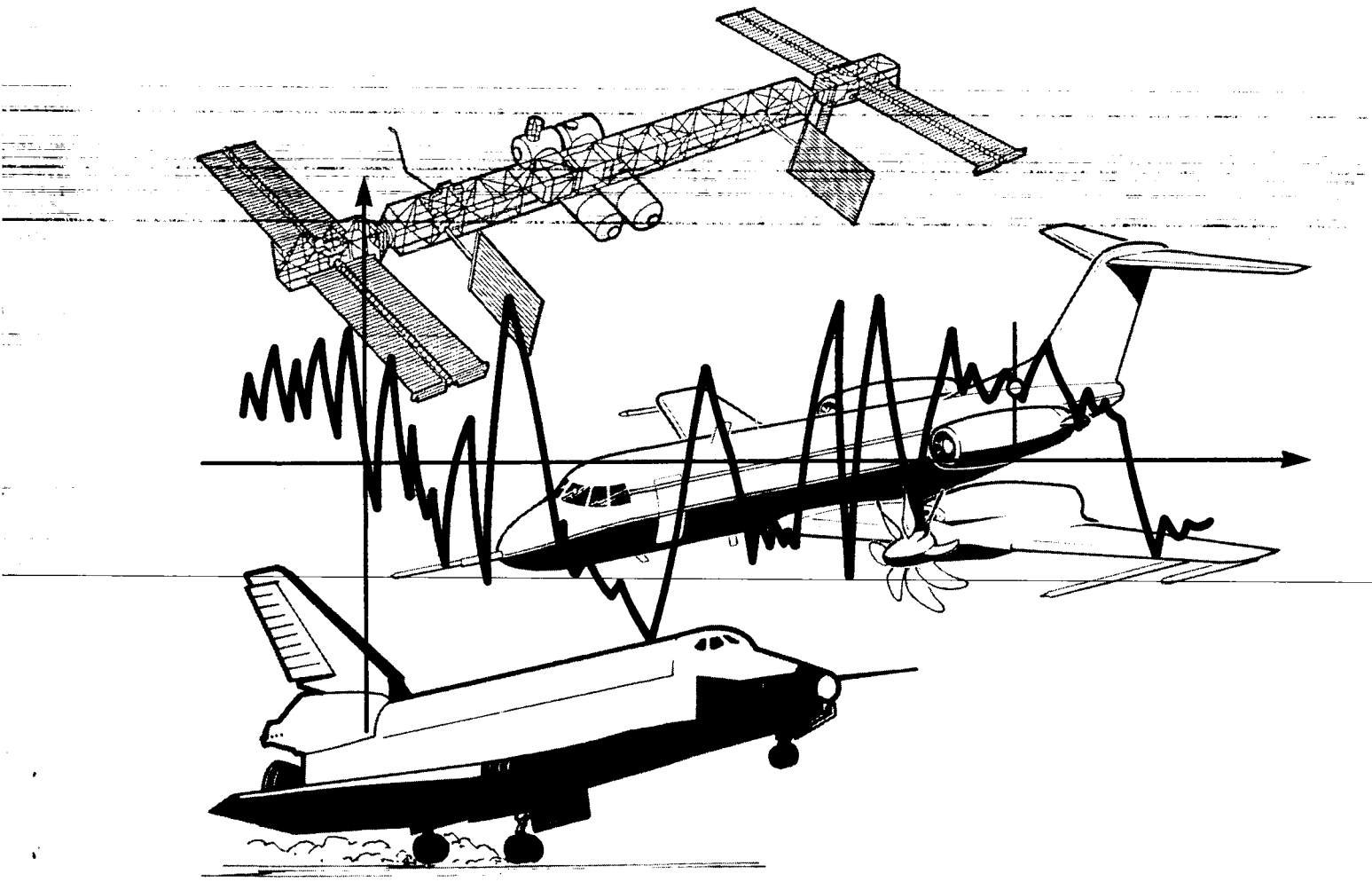

NASA

May 1988
Lewis Research Center

NASA Technical Memorandum 100279

Structural Dynamics Branch Research and Accomplishments for FY 1987

Lewis Research Center
Cleveland, Ohio

May 1988

National Aeronautics and
Space Administration

Scientific and Technical
Information Branch

Introduction

This document summarizes some of the technical accomplishments of the Structural Dynamics Branch of NASA Lewis Research Center for fiscal year 1987. Included is the work of our in-house researchers, contractors, and grantees.

The Structural Dynamics Branch conducts research dealing with advanced propulsion and power systems as well as precision mechanical systems. Our work directly supports NASA's turboprop, space experiments, space shuttle main engine, National Aerospace Plane (NASP), space station, and space power programs. This work can be broadly classified into four major areas: turbomachinery aeroelasticity, turbomachinery vibration control, dynamic systems response and analysis, and computational structural methods.

In aeroelasticity, we develop improved analytical and experimental methods for minimizing flutter and forced vibration response of aerospace propulsion systems. Work elements include classical (frequency domain) methods, computational (time domain) methods, experimental methods, and application studies (turboprop, turbofan, turbopump, and advanced core technology).

In vibration control, we conceive, analyze, develop, and demonstrate new methods to control vibrations in aerospace systems to increase life and performance. Work elements include active methods, passive methods, forcing functions, and application studies (electromagnetic dampers, magnetic bearings, and cryoturbomachinery).

Dynamic systems work is directed toward analyzing and verifying the dynamics of interacting systems as well as developing concepts and methods for motion control in microgravity environments. Work elements include microgravity robotic systems, parameter identification methods, and application studies (space lab robots, SP100 engines, NASP sealing, tethered satellite dynamics).

Our computational methods work is directed toward exploiting modern computer science to fundamentally improve the usage of computers in the solution of structural problems. Work elements include algorithms for modern computing, engineering data analysis, parallel architecture computers, and application studies (parallel finite element methods, animation, transputer lab studies, and transient analysis methods).

The microgravity robotic systems and the computational structural activities are newer work areas for us. These newer areas come from our increasing emphasis on either fundamentally generic work or space related research as opposed to our traditional aeronautics-based research activities.

Also, we have shifted the emphasis of our program for this next year. We have expanded our efforts in electromagnetic damping technology and magnetic bearing technology for controlling rotor systems vibrations. We have made a major commitment to developing active control methods for transient and steady-state rotor dynamics, with particular emphasis on magnetic bearing systems. Also, we have expanded our efforts in time domain aeroelastic computations. We have concurrently decreased work on passive dampers, traditional rotor dynamics modeling, and frequency domain methods for aeroelasticity. I anticipate that next year's report will reflect these changes in emphasis.

L.J. Kiraly
Branch Manager

Contents

Active Control of Transient Rotordynamic Vibration

The control of rotordynamic vibration is a key consideration in designing jet engines and rocket engine pumps for increased efficiency and reliability. Passive devices such as squeeze film dampers have previously been employed for nominal unbalance loads; however, their effectiveness under transient loads (e.g., blade loss) is poor. The objective of this research was to develop an active vibration control technology to suppress transient rotordynamic vibrations by utilizing piezoelectric pushers as actuators.

The steps in accomplishing this research were to

(1) Identify structural and electrical characterizations of the piezoelectric pushers via testing

(2) Formulate active control algorithms incorporating the structural characterization from (1)

(3) Design and construct the electrical circuits required for the control algorithm in (2)

(4) Verify the effectiveness of the active control system under steady-state conditions

(5) Verify the effectiveness of the active control system under transient loading (blade loss)

Since nearly all active vibration control theories are based on utilizing control forces, whereas the tests showed that the piezoelectric pushers yielded "control displacements," several new theories were developed. These consisted of optimal control, pole placement, and uncoupled velocity feedback schemes. The velocity feedback and optimal control approaches were checked by computer simulation of blade loss on the transient rotordynamics rig. The runs confirmed the theories, although some numerical difficulties were encountered when the actuator weight matrix of the objective function in optimal control was allowed to approach the null matrix. A general feedback device was conceptualized for application to all linear control schemes. The instrument was then designed and debugged of assembly errors.

Tests were performed with the velocity feedback scheme installed in the rig. The closed-loop system initially had a high-frequency (500 to 1500 Hz) instability problem that was circumvented by insertion of a 2-Hz bandpass filter in the loop. The center frequency was at the rotor speed frequency. This modification provided very good results under steady-state operating conditions as illustrated by figures 1(a) and (b).

Several attempts were made to utilize the active control circuit during transient blade loss tests; however, no significant reduction in vibration was detected between the controlled and uncontrolled tests. The tracking filter has a slow response time for changes in the vibration waveform; therefore, although the controlled vibrations were significantly smaller than their uncontrolled counterparts after several seconds past the transient, the controlled and uncontrolled vibrations during the transient were almost identical.

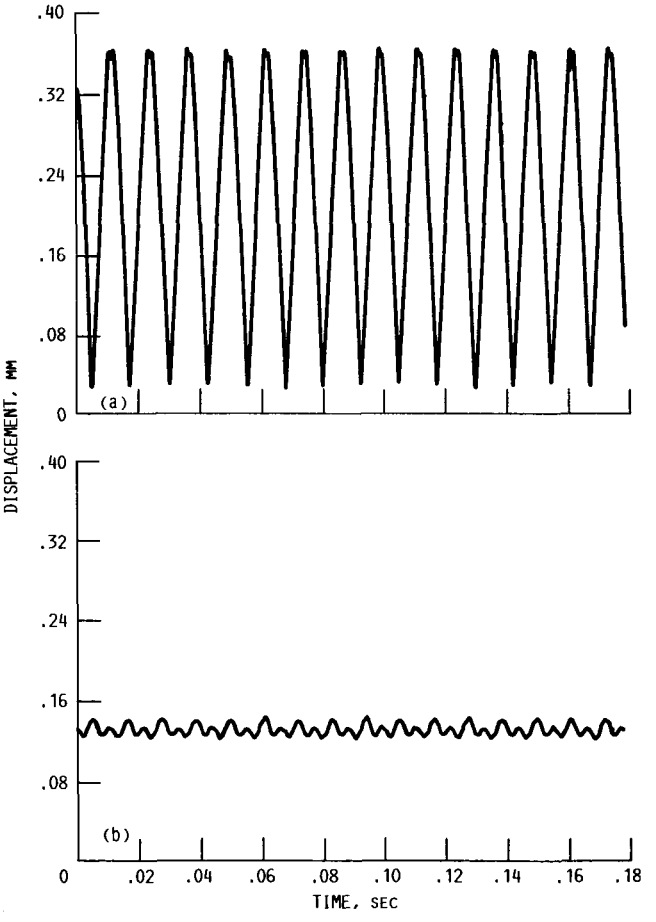

(a) Without instability control.
(b) After insertion of a 2-Hz bandpass filter to damp vibration.

Figure 1.—Vibration at the outboard bearing housing horizontal probe; speed, 5200 rpm.

Researchers: A.B. Palazzolo (Texas A&M), A.F. Kascak (AVSCOM), G.T. Montague (Sverdrup), E.H. Meyn and J.J. Ropchock (NASA Lewis), and R. Lin (Texas A&M).

Active Control of Transient Rotor Vibration

Rotating machinery may experience dangerously high dynamic loading because of the sudden mass unbalance associated with blade loss. The objective of this research was to investigate the application of active vibration control methods to suppress rotor vibrations caused by sudden mass unbalance.

A computer model was formed to simulate the NASA rotordynamics rig (fig. 2) subjected to sudden unbalance, with and without control. The simulation model included a form of optimal control in modal space with output feedback, pole placement with output feedback, nonlinear on-off control dependent on the sign of the velocity, and nonlinear on-off control dependent on shaft position. The effectiveness of each algorithm was examined in terms of vibration reduction and required actuator force levels. Simulations were made at both 5730 and 12 500 rpm.

The results of this research showed

(1) Optimal control, pole placement, and on-off velocity-dependent control significantly suppress transient vibrations caused by sudden unbalance. On-off position-dependent control was not effective in suppressing vibration. The most effective method appears to be optimal control, based on the computer runs made for this research.

(2) Sensors must be located at all actuator positions (i.e., collocated), in order to avoid instability in the closed-loop system. This is referred to as "spillover" of the higher, uncontrolled modes in a reduced order model.

(3) The best results obtained at 5730 rpm (600 rad/sec) were for the case of optimal control with collocation. Figure 3 contains results for this case. The vibrations at the actuator locations are less than 5.5 mils (peak to peak), and the actuator forces are less than 125 N (zero to peak).

The researchers are currently conducting experiments at NASA Lewis to verify the simulation results presented in this research.

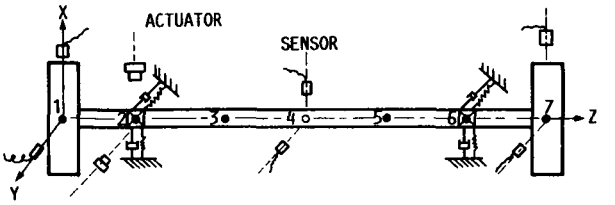

Figure 2.—Schematic diagram for the seven mass rotor model of the rotordynamics rig.

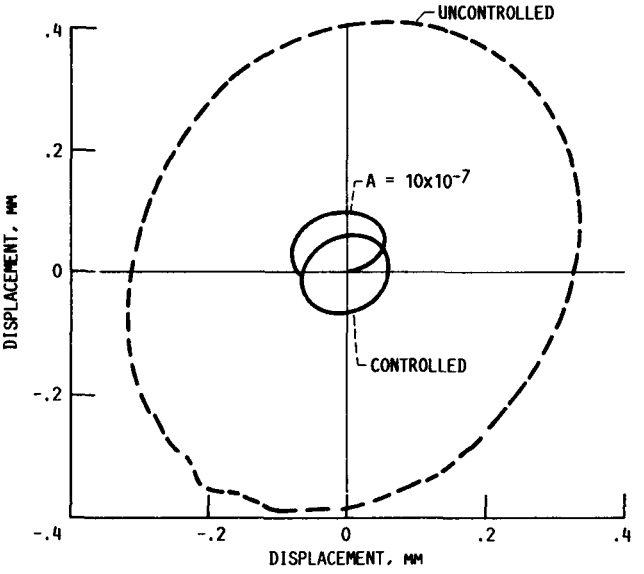

Figure 3.—Seven mass rotor test results.

Researchers: A.F. Kascak (AVSCOM) and A.B. Palazzolo and R. Lin (Texas A&M).

Analytical Flutter Investigation of a Composite Propfan Model

A theoretical model and computer program called ASTROP has been developed for predicting subsonic bending-torsion flutter of propfans. One version of the code, ASTROP2, uses two-dimensional, subsonic, unsteady (cascade) aerodynamics, and another version, ASTROP3, uses three-dimensional, subsonic, steady and unsteady (cascade) aerodynamics. Both versions use a finite element model (NASTRAN) to represent the blade structure.

Theoretical results have been correlated with flutter data for a wind tunnel propfan model with composite blades. Figure 4 shows calculated and measured flutter speeds for four and eight blades. The calculations are from ASTROP3 and include the effects of centrifugal loads and steady-state airloads. The theory does reasonably well in predicting the flutter speeds and the slopes of the boundaries. However, the difference between the calculated and measured flutter Mach numbers for the four-blade case is greater than for the eight-blade case. This discrepancy implies that the theory may be overcorrecting for the aerodynamic cascade effects for four blades. These results (fig. 4) are for a blade pitch angle of 61.6°. Similar comparisons (not shown) that were made at blade angles of 56.6° and 68.4° showed about the same agreement. Calculated interblade phase angles at flutter (not shown) also compared well with measured values. However, calculated flutter frequencies were about 8 percent higher than measured. Both theory and experiment showed that increasing the number of blades on the rotor and increasing the blade pitch angle destabilize the rotor.

Analysis showed that the flutter speed predicted by two-dimensional aerotheory is less accurate than that predicted by three-dimensional theory. Hence, final design calculations should be done with three-dimensional analysis. In addition, the influence of steady-state aerodynamics on the blade-deflected steady-state geometry, blade mode shapes, and flutter speed is significant in some cases. Thus, the steady-state aerodynamics should be included in final design calculations.

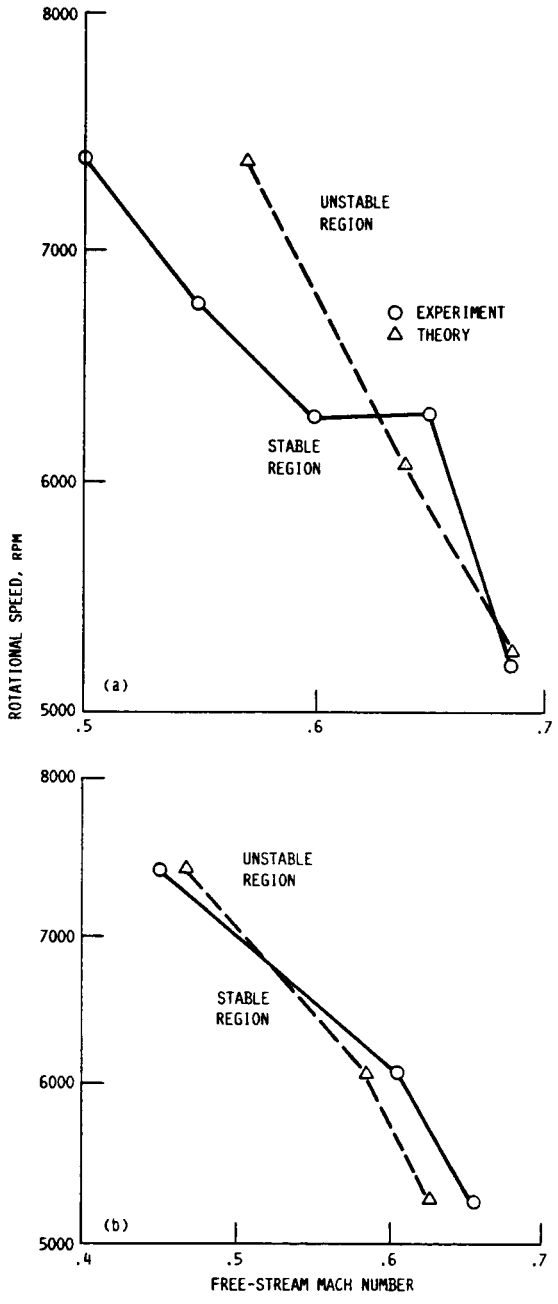

(a) Four blades.
(b) Eight blades.

Figure 4.—Comparison of measured and calculated flutter boundaries for the SR3C–X2 propfan model.

Researchers: K.R.V. Kaza and O. Mehmed (NASA Lewis), G.V. Narayanan (Sverdrup), and D.V. Murthy (Univ. of Toledo).

Analytical and Experimental Investigation of Mistuning in Propfan Flutter

An analytical and experimental investigation of the effects of mistuning on propfan subsonic flutter has been performed. The analytical model is based on the normal modes of a rotating composite blade and on three-dimensional unsteady lifting surface (cascade) aerodynamic theory that was developed for this analysis. A mistuned wind tunnel model was constructed by alternately mounting two sets of composite blades (SR3C–X2 and SR3C–3). These blades were molded from graphite-ply—epoxy-matrix laminates with different ply directions (fig. 5). The analytical model was validated for selected cases by comparing predicted and measured flutter characteristics of the (mistuned) wind tunnel rotor (SR3C–X2 and SR3C–3).

Figure 6 shows a typical comparison of measured and calculated flutter boundaries for a 61.2° blade pitch angle. Results for both the tuned rotor, SR3C–X2, and the mistuned rotor, SR3C–X2 and SR3C–3, are included in the figure. As can be seen from the figure, the correlation between theory and experiment is good. Calculated flutter frequencies (not shown) are approximately 3 to 6 percent higher than those measured.

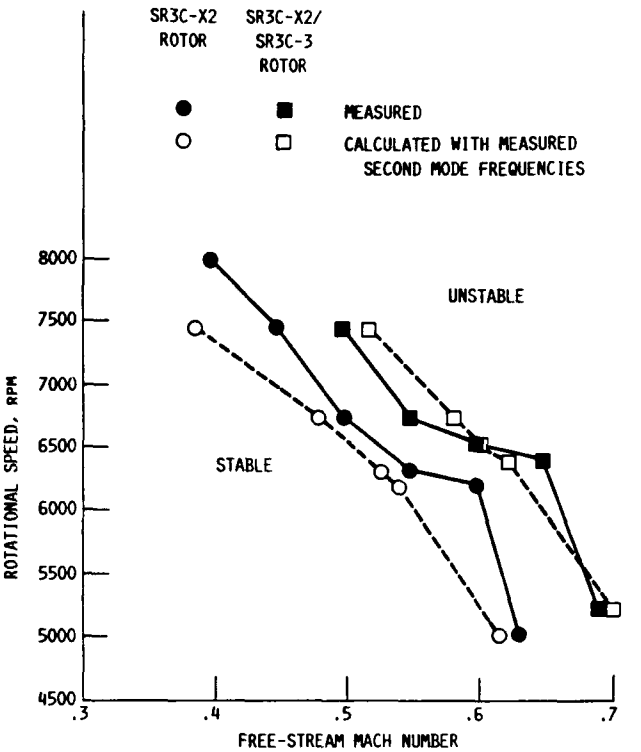

Figure 6.—Measured and calculated flutter boundaries.

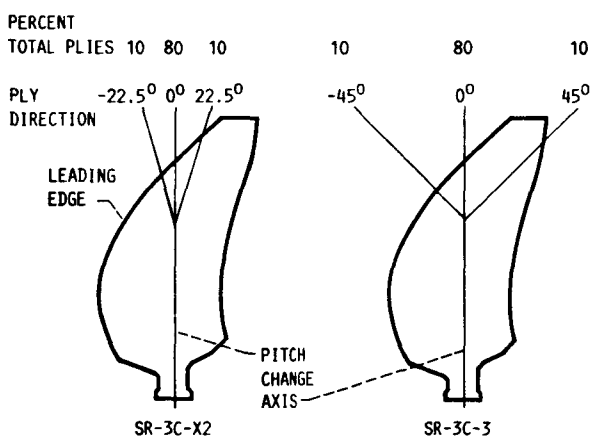

Figure 5.—Blade ply directions of composite blades used for the mistuned wind tunnel model.

After validating the code, additional parametric studies were conducted. The results showed that the combined mode shape, frequency, and aerodynamic mistuning can have either a beneficial effect or an adverse effect on blade damping, depending on the Mach number range. The results also indicated that alternate frequency mistuning does not have enough potential for it to be used as a passive flutter control in propfans similar to the one tested in the present investigation.

Finally, from theoretical and experimental results, it is concluded that a laminated composite propfan blade can be tailored to optimize its flutter speed by properly selecting the ply angles.

Researchers: K.R.V. Kaza and O. Mehmed (NASA Lewis), M. Williams (Purdue), and L.A. Moss (Sverdrup).

A Technique for the Prediction of Airfoil Flutter Characteristics in Separated Flow

A solution procedure is presented for determining the one- or two-degree-of-freedom flutter characteristics of arbitrary airfoils at large angles of attack including separated flow. The fluid model is based on two-dimensional unsteady compressible Navier-Stokes equations in a body-fitted coordinate system. The solid-fluid equations are simultaneously integrated in time. The analytical model and solution procedure are validated by applying them to special cases. Finally, promising results have been obtained for predicting the phenomenon of dynamic stall flutter.

Figure 7 illustrates the capability of the Navier-Stokes solver in highly separated flows by showing measured and calculated lift, drag, and moment hysteresis loops for a NACA 0012 airfoil oscillating in pitch. The mean angle of oscillation is 15°, while the amplitude of the oscillations is 10°. The reduced frequency, based on semichord, is 0.151 and the free-stream Mach number and Reynolds number, respectively, are 0.283 and 3.45 million. Figure 7 shows that the theory correctly predicted the linear increase in lift during upstroke, the dynamic stall (vortex effects) that causes rapid variations in lift, drag, and moment, and the post-stall recovery phase of the flow during the down stroke. The ability of the flow solver to capture much of the dynamic stall features and the good agreement between theory and experiment establish the confidence in the capability of this code for stall flutter predictions. Consequently, this flow solver can be used to generate similar hysteresis loops for the airfoils employed for propfans. Then these loops can be synthesized (in the same way the experimental loops would be synthesized), reducing the reliance of the stall flutter analysis on the availability of a large body of experimental data.

After validating the analytical model for classical flutter solutions, two sets of stall flutter calculations were performed for flow over the NACA 0012 airfoil at a Mach number of 0.3 and a Reynolds number of 9 million. In the first set (fig. 8) the airfoil was perturbed from a steady angle of attack of 15°, and in the second set it was perturbed from 23.82° (not shown here). The dimensionless speed was varied from 4 to 8. In both sets the airfoil was stable when the speed was 4 and was unstable when the speed was 8. To make sure the flutter response was not a classical one, the calculations were repeated at lower angles of

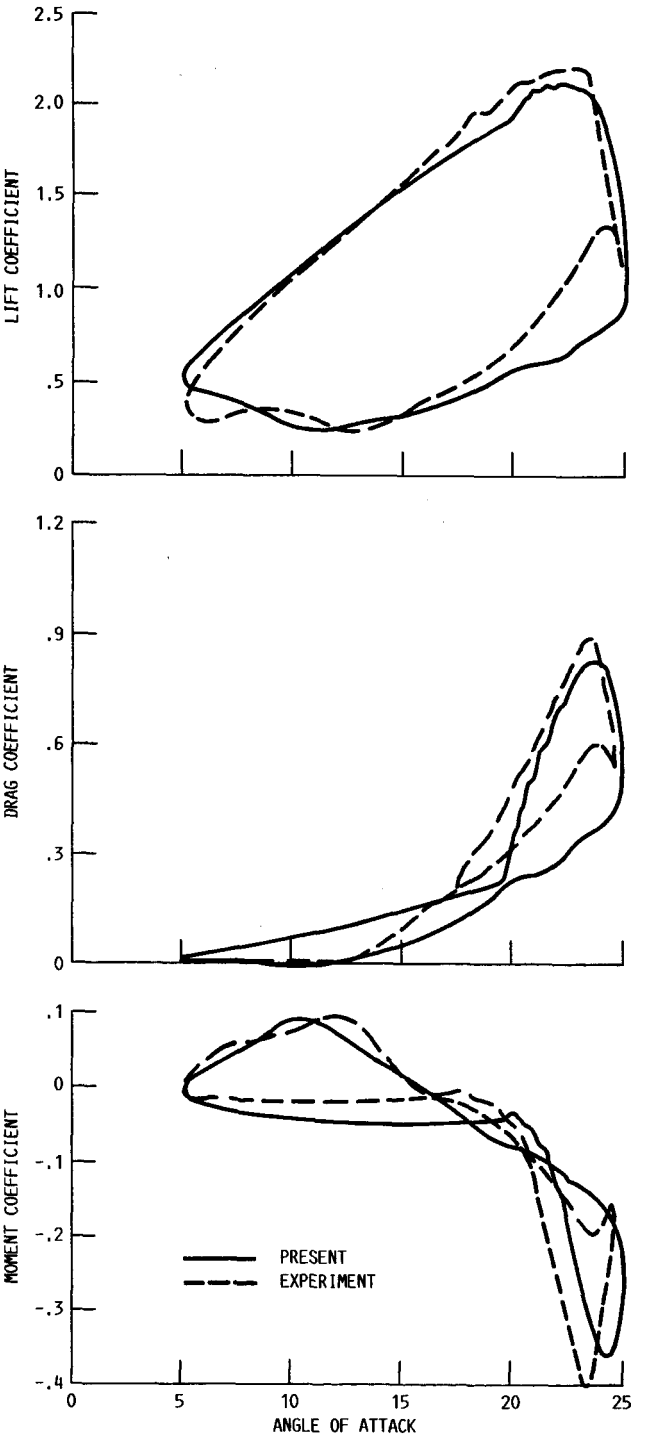

Figure 7.—Comparison of theoretical and experimental lift, drag, and moment hysteresis loops for unsteady airloads on the NACA 0012 airfoil.

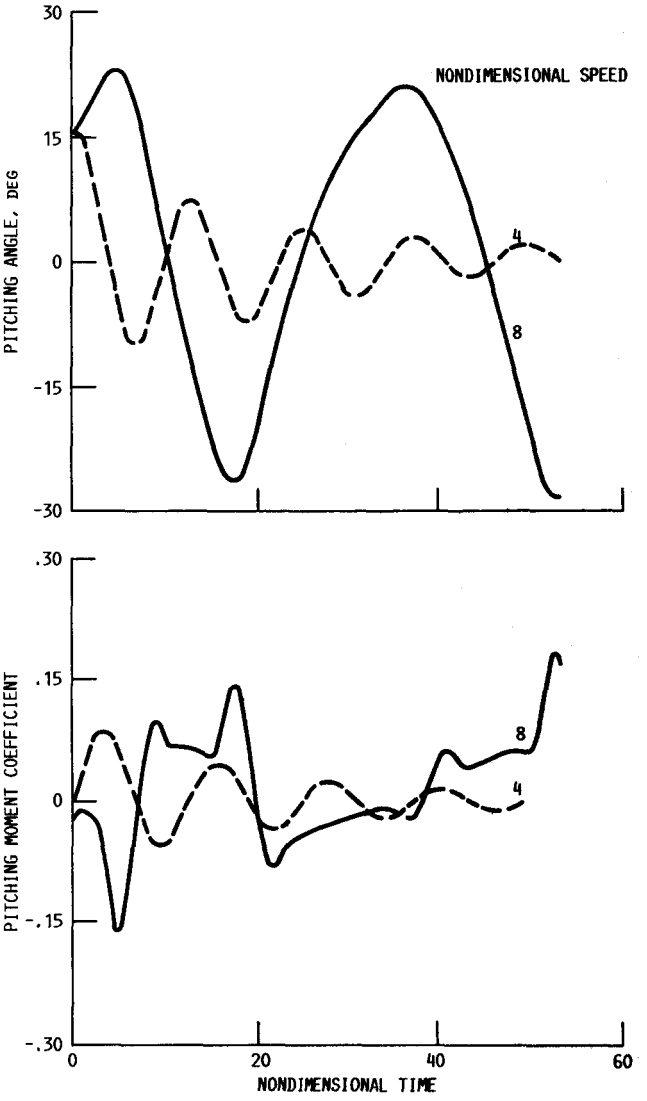

Figure 8.—Stall flutter calculations of time response for pitching and plunging NACA 0012 airfoil.

attack (between 8° and 10°), but no flutter was found. Thus, it is concluded that the growing response in figure 8 was triggered by the stalled flow over the airfoil at high angles of attack.

In summary, an analytical model for predicting the dynamic stall flutter speed of oscillating airfoils has been developed. This is a first step in modeling a complex separated flow phenomenon over oscillating airfoils, propfans, and turbofan rotors by exploiting the capabilities of supercomputers. The results should be repeated with different turbulence models and more refined grid geometry to assess their effects.

Researchers: J. Wu (Georgia Tech.), K.R.V. Kaza (NASA Lewis), and L.N. Sankar (Georgia Tech.).

A Computational Procedure for Automated Flutter Analysis

Classical flutter is a significant factor in the design of propfan blades and other types of turbomachinery blading. An automated flutter analysis capability is essential for automated design of propfan and turbomachinery blades using optimization techniques employing flutter constraints. It is also desirable for the analysis to be computationally efficient in order to keep the central processing unit (CPU) and the turnaround times within reasonable limits.

The conventional flutter analysis procedure casts the equations of motion as a complex linear eigenvalue problem. The solution consists of an inner-outer iteration loop to obtain the flutter Mach number M and frequency. The inner iteration loop matches the assumed frequency ω to the calculated frequency while the outer loop iterates on the Mach number to obtain a zero effective damping. This double iteration loop is computationally expensive. In addition, the need to track several eigenvalues through possible crossovers has been a stumbling block in the development of a reliable automated procedure.

This work explores an efficient and automated procedure that replaces the costly inner-outer double iteration loop with a single iteration loop. The need to track the eigenvalues is also avoided. This is accomplished by viewing the flutter problem as a complex, implicit double eigenvalue problem and directly solving for the flutter Mach number and the flutter frequency by a quasi-Newton determinant iteration. The flutter eigenvalues are never calculated, and the avoidance of eigenvalue tracking makes true automation possible.

Two nonlinear equations are solved to obtain the flutter Mach number and the flutter frequency, and the flutter mode is obtained very efficiently with the information available from the final iteration. An accurate approximation to the Jacobian matrix, which makes the iterative process very efficient, is a new feature of this technique. The Jacobian matrix is approximated from the approximate derivatives of the system flutter matrix. The derivatives of the system flutter matrix are subsequently updated only in the direction of the last iteration step and are kept constant in the direction orthogonal to the last step.

The technique developed is tested by applying it to the flutter analysis of a propfan model at a number of rotational speeds. A tuned rotor, as well as an alternately mistuned rotor, are considered. The flutter boundaries obtained are in excellent agreement with those obtained using the conventional procedure.

TABLE I.—PROGRESS OF ITERATION

Count	Conventional procedure		Present procedure	
	M	ω, Hz	M	ω, Hz
1	0.500	310.0	0.500	310.0
2	↓	267.5	.499	310.0
3	↓	268.9	.500	313.0
4	↓	268.9	.701	289.7
5	.700	268.9	.590	287.7
6	↓	299.8	.641	293.6
7	↓	298.9	.642	294.1
8	↓	298.9	.641	294.1
9	.616	286.3	[a].641	294.1
10	↓	290.1		
11	↓	290.5		
12	↓	290.4		
13	.640	292.9		
14	.640	293.9		
15	.640	294.0		
16	.641	293.9		
17	.641	294.1		
18	[a].641	294.1		

[a]Converged.

The progress of iteration for this technique is compared in table I with that of the conventional procedure for a typical case. Figures 9 and 10 compare the efficiency of this technique with that of the secant method. The wide range of initial guesses for convergence is also depicted in the figures.

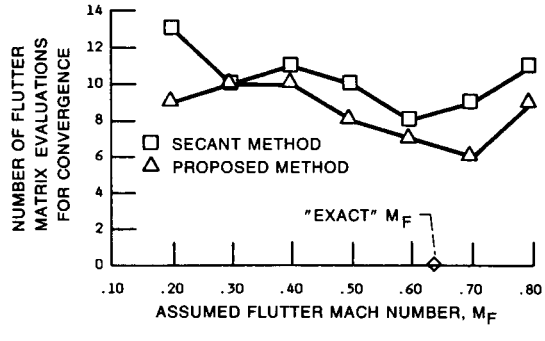

Figure 9.—Comparison of present iteration technique with secant method for convergence of direct solution for various initial guesses at flutter Mach number.

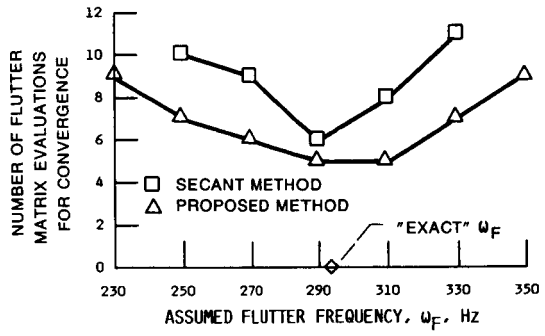

Figure 10.—Comparison of present iteration technique with secant method for convergence of direct solution for various initial guesses at flutter frequency.

The results obtained show that the direct solution procedure using the Jacobian approximation developed facilitates the automated flutter analysis of propfans in addition to contributing to the efficient use of computer time as well as analyst's time.

Researchers: D.V. Murthy (Univ. of Toledo) and K.R.V. Kaza (NASA Lewis).

Hub Flexibility Effects on Propfan Vibration

The significance of hub flexibility in the nonlinear static and dynamic analyses of advanced turboprop blades was assessed. To date, most analyses have assumed that the blades are rigidly attached at their base. This simplification makes blade modeling easier, but does not allow for the effect of hub flexibility to be included in the analysis. The objective of this study was to determine the effect of hub flexibility on propfan steady-state displacement, frequencies, and mode shapes.

The effect of hub flexibility was evaluated by performing steady-state displacement and frequency analyses on the GE–A7–B4 unducted fan (UDF) blade. Selection of this blade was based on the availability of an effective hub stiffness, characterized by a 6 by 6 stiffness matrix corresponding to the six degrees of freedom of the hub attachment point (fig. 11).

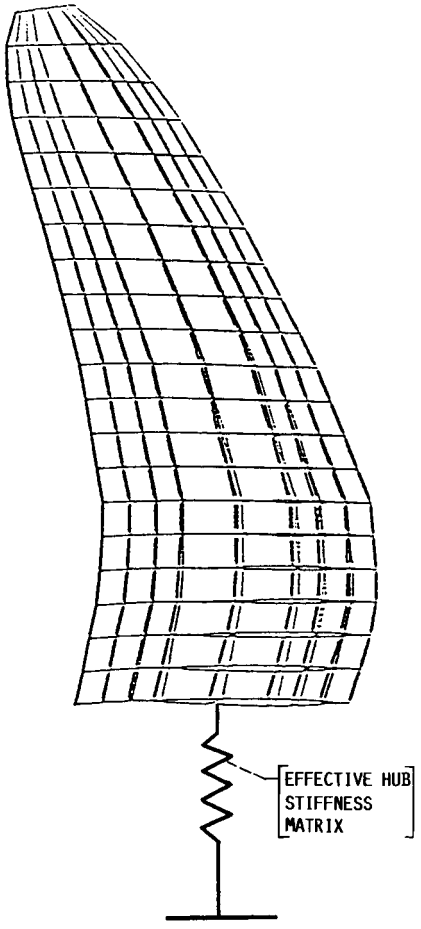

Figure 11.—Finite element model of GE–A7–B4 unducted fan blade and effective stiffness matrix.

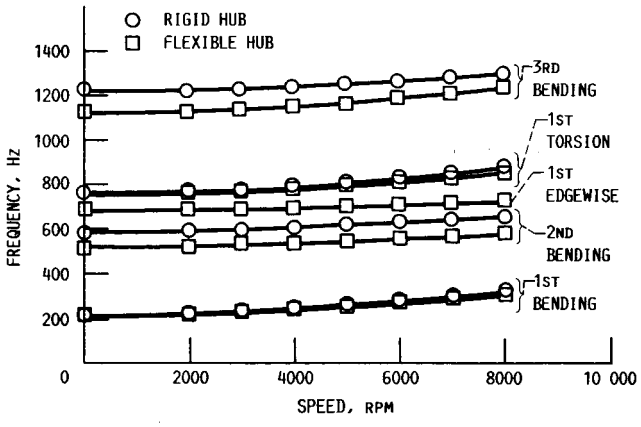

Figure 12.—GE–A7–B4 fan blade modal frequencies. Rigid hub versus flexible hub.

In order to assess the effects of hub flexibility, a series of large displacement and dynamic analyses were performed at various rpm's using MSC/NASTRAN's solution sequences 64 and 63, respectively. While most MSC/NASTRAN solution sequences allow for the modification of the global stiffness matrix with stiffness coefficients, there was no direct method to apply the hub stiffness matrix to the blade's finite element model in a solution 64 large displacement analysis. Therefore, a procedure was developed and verified, allowing for the coupling between a symmetric stiffness matrix and a NASTRAN finite element model in a solution 64 large displacement analysis. Although this procedure was demonstrated using an analytically derived effective hub stiffness, it is equally applicable for an experimentally obtained hub stiffness.

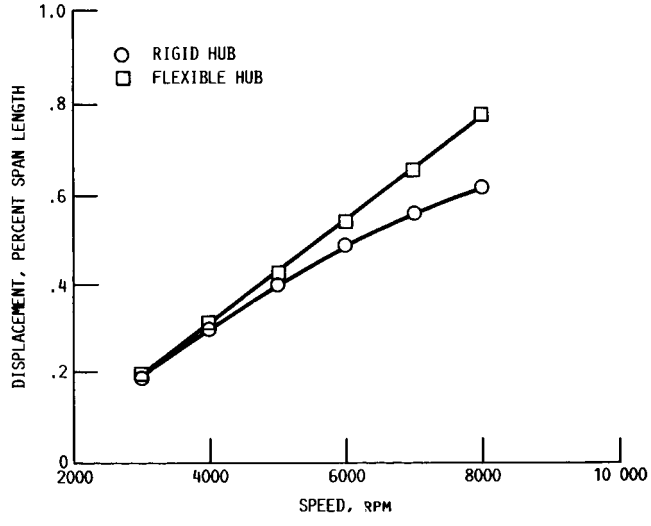

Figure 13.—GE–A7–B4 fan blade leading-edge tip displacements. Rigid hub versus flexible hub.

The effect of hub flexibility on steady-state displacement and frequencies has been shown to be significant for the GE–A7–B4 UDF blade. A drop in the second bending, third bending, and first edgewise modal frequencies may have a significant impact on any aeroelastic analysis conducted on the blade (fig. 12). In addition, at speeds greater than 4000 rpm, the influence of the flexible hub on the static displacement of the GE–A7–B4 becomes notable (fig. 13).

Overall, in order to insure accuracy in analyses of other propfan blades, hub flexibility should always be considered. If hub flexibility effects are not assessed, the accuracy of the results will be questionable.

Researchers: M.A. Ernst and C. Lawrence (NASA Lewis).

Identification of Structural Interface Characteristics Using Component Mode Synthesis

Large structural systems are often analyzed using component mode synthesis (CMS) techniques. CMS, which utilizes a reduced set of component modes to characterize the overall system behavior, is a widely accepted analytical tool for predicting coupled system response with increased modeling efficiency and flexibility. However, deficiencies in existing modeling techniques limit CMS's ability to adequately model the connections between components. Connections between structural components, and between components and ground, often are mechanically complex and, hence, very difficult to accurately model analytically. The influence that connections exert on overall system behavior can be profound because the connections alone determine the boundary conditions imposed on the system components. Thus, to refine the prediction of system behavior, improved analytical models for connections are needed.

Parameter identification (PID) can be used when experimental data are available from modal tests. Parameter identification improves modeling accuracy by reducing discrepancies between the measured characteristics of an actual physical system and those predicted by an analytical model of the system. An array of techniques is available to carry out the process of parameter refinement. Most involve the determination of a set of structural parameters that optimally minimize differences between experimental measured responses and the predicted responses.

This research explored the process of combining CMS and PID to improve analytical modeling of the connections in a component mode synthesis model. The approach used in this work involved modeling the components with either finite elements or experimental modal data and then connecting the components "physically" at their interface points. Experimentally measured response data for the overall system then were used in conjunction with PID to make improvements in the connections between components. The connection improvements were computed in terms of physical parameters to provide better understanding of the physical characteristics of the connections in addition to providing improved input for the CMS model.

The rotating structural dynamics rig (RSD) (fig. 14) was used to assess the procedures with actual experimental data. The objective of the parameter identification was to determine the stiffnesses of the squirrel cage bearing support that connects each end of the rotor to the support frame. To accomplish this, the RSD rig was divided in two components: the rotor support frame, and the rotor. In the system model, the support frame was represented by an experimentally verified finite element model while the rotor was represented by experimental modal data.

Researchers: C. Lawrence (NASA Lewis) and A.A. Hucklebridge (Case Western Reserve Univ.).

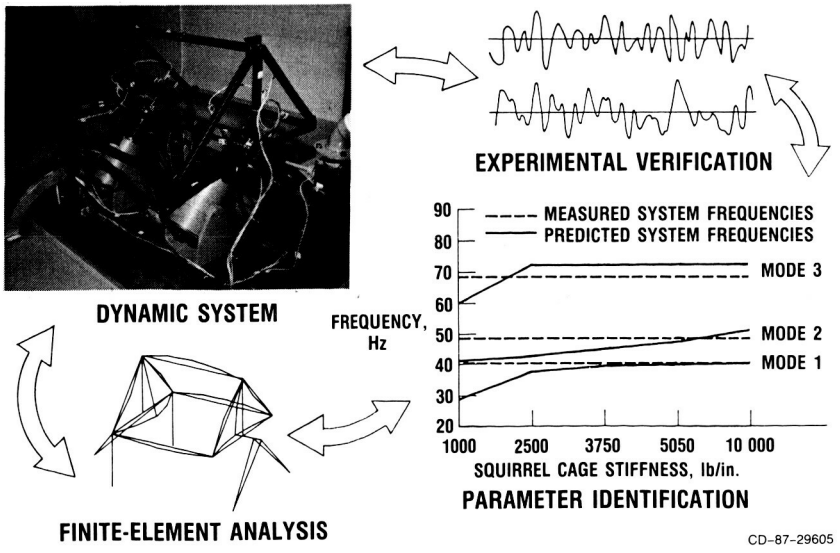

Figure 14.—Characterization of structural connections.

Stiffness and Damping of Tapered-Bore Seals

It is well known that annular seals (ring seals) can generate significant lateral forces and that these forces can strongly influence the dynamics of shaft systems. Analyses have predicted that tapered-bore seals (with the clearance diminishing in the flow direction) will have a higher stiffness than straight-bore seals for both incompressible and compressible fluids. Moreover, for compressible fluids, straight-bore seals can sometimes have a negative stiffness which is nearly always undesirable.

The apparatus (fig. 15) consists of a vertical shaft supported radially in two pairs of tapered-bore seals. A dynamic load was produced by unbalancing the shaft a known amount. Dynamic motions were measured by capacitance distance probes and a digital vector filter. These motions were input to the shaft equations of motion, which were then solved for stiffness and damping coefficients.

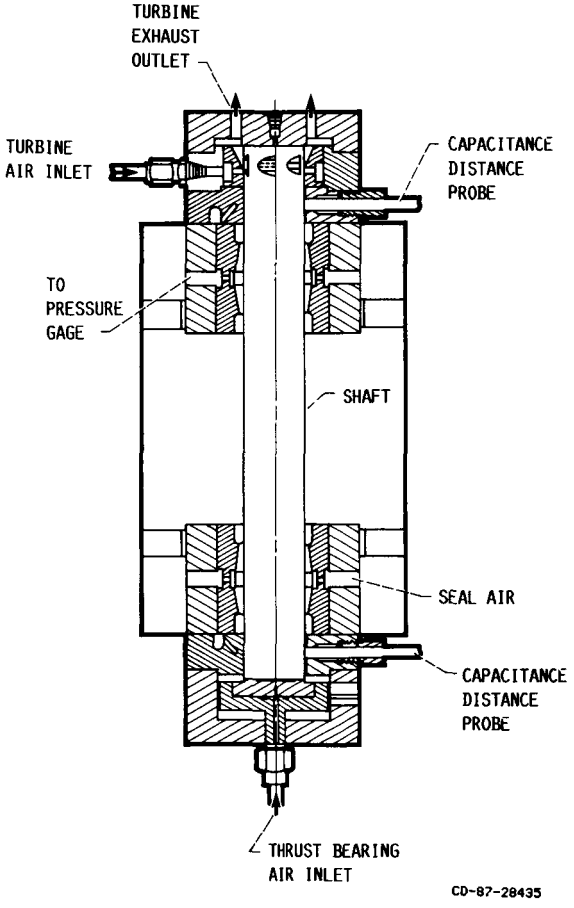

Figure 15.—Test apparatus for stiffness and damping coefficient measurement.

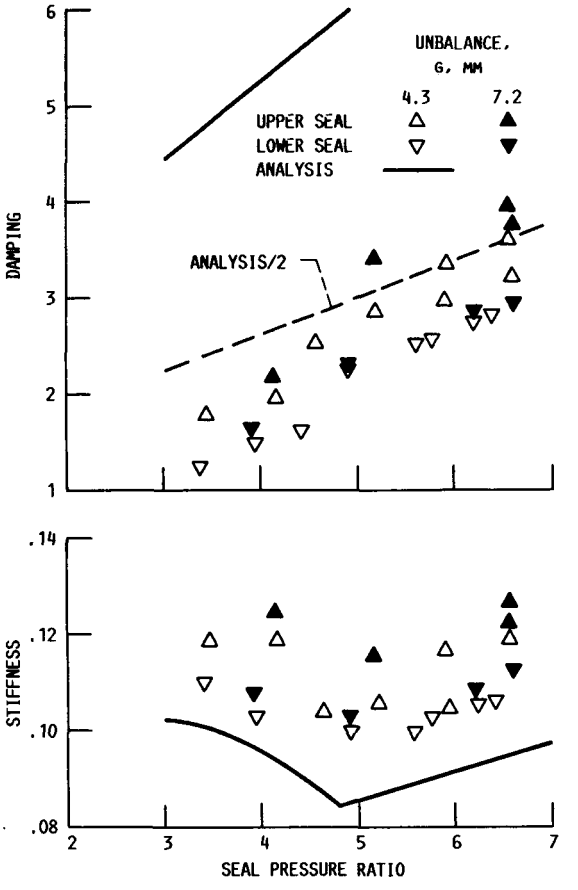

Figure 16.—Stiffness and damping for a tapered-bore ring seal; clearance, 0.026 mm.

Typical results are shown in figure 16. There is little change in stiffness (the lower part of the figure) with pressure ratio. This small variance is also predicted by analysis. Measured stiffness is somewhat higher than predicted, but within 30 percent.

Measured damping coefficients are much less than predicted. This is probably due to the limitation of the one-dimensional analysis used, which assumes flow in only the axial direction.

Researcher: D.P. Fleming (NASA Lewis).

Space Shuttle Main Engine Single-Crystal Turbine Blade Dynamics

There are many concerns surrounding the current space shuttle main engine (SSME) first-stage high-pressure-fuel turbopump (HPFTP) blades made of directionally solidified (DS) material. The blades' design life goal was 55 launches. However, the DS blades have been serviceable for only 2 to 5 launches. The blade life has been primarily influenced by fatigue cracking problems. One method of improving blade life is with a material substitution of single-crystal (SC) material. Past experience and current applications with commercial and military aviation have shown the feasibility of using SC material.

The purpose of this research was to predict the SC blade natural frequencies and find possible critical engine-order excitations. This study examined both the first- and second-stage drive turbine blades of the HPFTP (fig. 17). The effort was both experimental and analytical.

Experiments were used to validate the analytical procedures. Bench experiments for five SC blades at different crystal orientations were conducted to determine their nonrotating natural frequencies and mode shapes. Comparisons of these results with the analytical results were made to confirm the validity of the MSC/NASTRAN model.

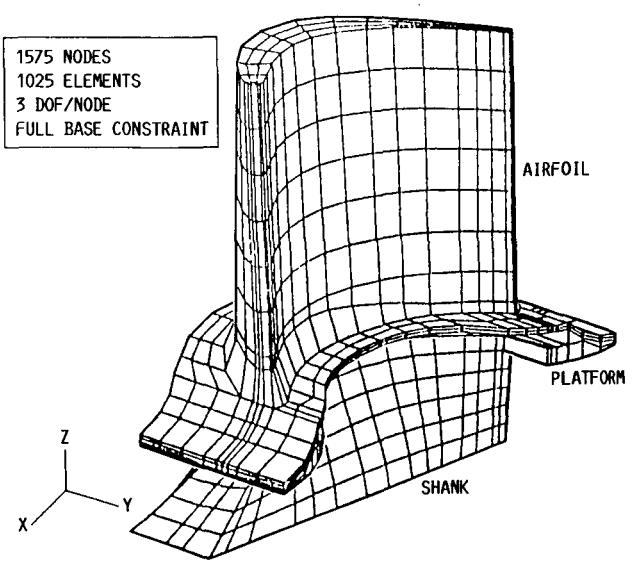

Figure 17.—MSC/NASTRAN finite element model.

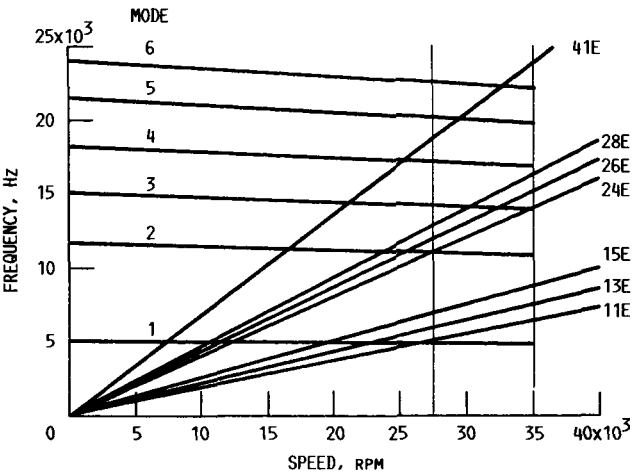

Figure 18.—Space shuttle main engine high-pressure-fuel turbopump—first-stage blade Campbell diagram.

The analytical effort examined the blades' dynamic characteristics with respect to crystal orientations under typical operating conditions. Additional investigations attempted to determine the optimum crystal orientation that would most effectively avoid critical engine-order excitations.

From a dynamics viewpoint, the SC blade is an improvement over the DS blade. No new engine-order interferences were introduced with the material substitution. The SC blade at nominal orientations was found to be better than the DS blade because the fourth mode interference was eliminated (fig. 18). The engine-order interferences within the SC blades' first three modes can be minimized by changing the crystal orientation. However, it was found that for any orientation, the third mode interference will exist.

Researchers: L.A. Moss and T.E. Smith (Sverdrup).

High-Pressure Turbine Blade Damper Optimization

Before 1975, turbine blade damper designs were based on experience and very simple mathematical models. Failure of the dampers to perform as expected showed the need to gain a better understanding of the physical mechanism of friction dampers. Over the last 10 years, research on friction dampers for aeronautical propulsion systems has resulted in methods to optimize damper designs.

The first-stage turbine blades on the SSME high-pressure oxygen pump have experienced cracking problems because of excessive vibration. A solution is to incorporate well-designed friction dampers to attenuate blade vibration. The subject study, a cooperative effort between NASA Lewis Research Center and Carnegie-Mellon University, represents an application of recently developed friction damper technology to the SSME high-pressure oxygen turbopump.

The major emphasis of the study was the contractor design known as the two-piece damper. Damping occurs at the frictional interface between the top half of the damper and the underside of the platforms of the adjacent blades. The lower half of the damper is an air seal to retard airflow in the volume between blade necks.

A bench test apparatus was developed to conduct an extensive set of experiments on the two-piece damper. The bench test apparatus was successful. The normal load was applied through a fishhook-pulley-weights system. The weights were varied from 0.25 to 70 lb. The blade support was tuned to simulate blade natural frequencies at pump operating temperatures and speeds (approx. 9.5 kHz for the edgewise bending mode). The excitation system consisted of an electromagnet and a small chip of transformer iron mounted on the blade. Blade response, measured with a miniature accelerometer, was up to 700g tip acceleration, 0.1-mil tip displacement, and 1700-psi stress at the crack location.

Analytical models were fit to the experimental data and used to extrapolate the results to pump operating conditions. These extrapolations show that the best thickness for the two-piece damper is 0.047 in. and that the performance can be improved by reducing width by 15 percent. However, it was found that the damper is working in the microslip regime (no gross slipping). The resulting reduction in stress is predicted to be approximately 3 to 1.

Whirligig testing at the contractor showed that tip clearance is the controlling parameter in blade vibration. In addition, testing of a tip damper showed excellent performance characteristics.

In summary, the two-piece damper is predicted to be a modest microslip damper. The damper performance at pump conditions should be dependent on tip clearance conditions. A tip damper was found to be an excellent performer.

Researchers: R.E. Kielb and E.H. Meyn (NASA Lewis).

Impact Damper Behavior and Performance

The impact damper (shown in schematic form in fig. 19) is a very simple device that can produce high damping through inelastic collisions over a wide range of frequencies in vibrating systems. But it is not easy to analyze because the inelastic impacts of the "impactor" on the walls of its cavity make the system nonlinear. Fifty years of study of special cases have failed to produce an overall picture of the complex behavior of this physically simple system. Predictions of its damping ability have been limited to narrow regimes of its behavior.

The present study has utilized a time-history solution of the motion of the system for the situation of the oscillator in free decay. The behavior of the impactor depends strongly on oscillator amplitude, and a free decay can sample the full range of possible behavior, which ranges from an infinite number of impacts per cycle at high oscillator amplitude to no impacts at a sufficiently small amplitude. This overall picture was not provided by previous steady-state studies.

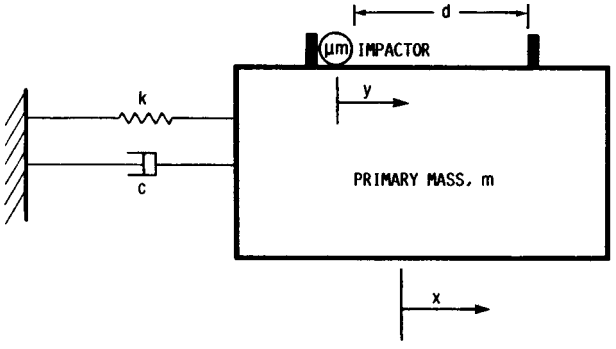

Figure 19.—Impactor-damped harmonic oscillator.

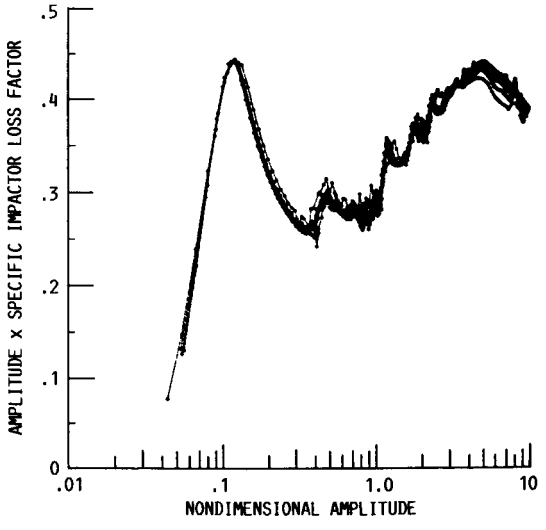

Figure 20.—Amplitude times specific loss factor as function of amplitude.

The damping values were calculated, and, because of the way the system equations were nondimensionalized, they have the widest possible applicability. Figure 20 shows how one measure of damping, the loss factor (the fraction of vibrational energy lost per radian of vibration), depends on the nondimensional amplitude of vibration. The rather complex variation of damping with amplitude results from the varying numbers and times of impacts that occur within a vibration cycle. Figure 21 shows the times of impacts (plotted as the oscillator phase at each impact) as a function of amplitude. This rather striking plot shows behavior ranging from regions of comparatively regular impacts (such as two impacts in every half-cycle), which appear as bold lines, to regions that actually meet the definition of chaotic behavior (nonperiodic, yet bounded motion), where the impact points appear randomly scattered.

Following completion of forced-response studies now in progress and of a planned demonstration of impact damping in a rotating system (previously tried unsuccessfully by others) with some fresh concepts for preserving impactor motion in spite of high centrifugal forces, the impact damper could see application in advanced turboprops or in fans of commercial engines. If successful, this would permit higher performance because of the removal of vibration constraints.

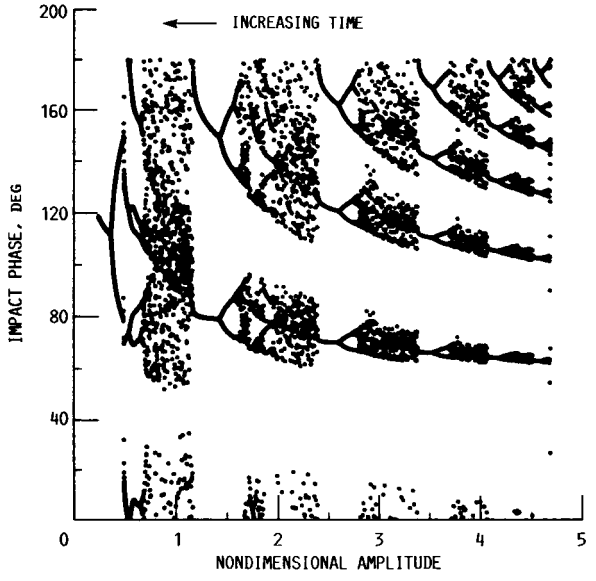

Figure 21.—Impact phase (measured from oscillator zero crossing) as function of oscillator amplitude.

Researchers: G.V. Brown (NASA Lewis) and C.M. North (Rose-Hulman).

Transputer Algorithms for Structural Dynamics Problems

Computer codes have been written for the parallel solution of systems of linear equations arising from the modeling of transient rotor dynamics and for the explicit time integration of finite element equations. The codes have been written in the OCCAM computer language for implementation on the transputer computer system.

In the analysis of nonlinear rotordynamics problems, the application of a Newton-Raphson iterative technique to the equilibrium equations leads to a system of block tridiagonal linear equations. To solve these equations, the preconditioned conjugate gradient method was chosen for the parallel computer implementation because it requires less data transmission than traditional direct solution methods such as Gauss elimination.

For a test problem with the dimension of the blocks set at four and with a various number of blocks, the parallel algorithm running on computer with two external processors ran approximately twice as fast as the sequential code.

An explicit finite element time integration program was parallelized by partitioning the nodes into groups that could be updated by different processors of the computers over a time step. The code was run on a parallel processing computer system with as many as ten external processors in a ring configuration. Test results indicate that speed can be increased by a factor of three by appropriately balancing the work load among the processors.

Figures 22 and 23 detail a three-processor implementation of the algorithm. The host processor, Processor 1, coordinates the activities of the other processors. In figure 22, preconditioning steps are shown, and, in figure 23, iterative procedures are shown. Blocks of code, representing portions of the block tridiagonal matrix are distributed to an array of processors, two of which are shown in the figures. Other, potentially more efficient, ways of distributing the code are being investigated.

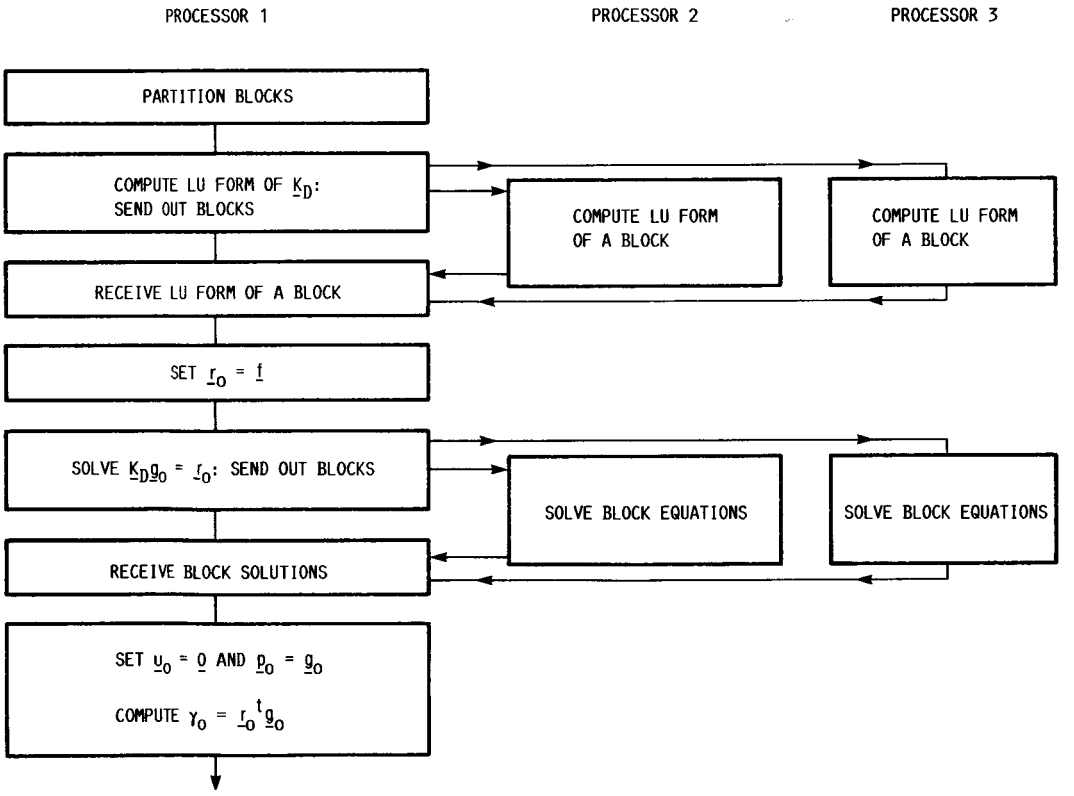

Figure 22.—Preconditioning for conjugate gradient integration.

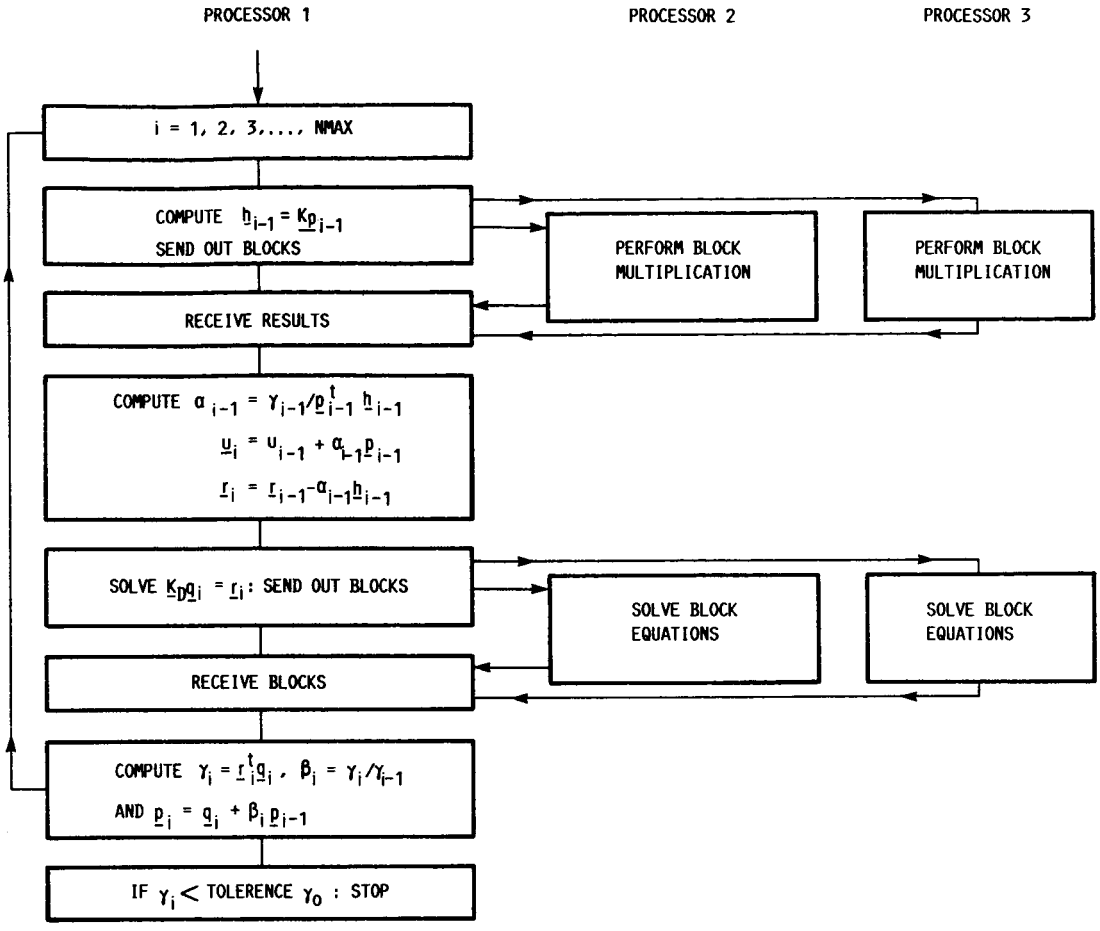

Figure 23.—Iteration loop for conjugate gradient integration.

Researchers: P. Smolinski (Univ. of Pittsburgh) and L.J. Kiraly (NASA Lewis).

A Model for Evaluating Multiprocessor Architectures

Computer architecture design has, for the most part, been done on an ad hoc basis. Different interconnections between elements and levels of memory hierarchy have been suggested based on the experience of the designer and on results from other similar architectures.

Computer architectures may be described by characteristics coming from two separate classes—the class of quantitative characteristics such as size and speed and the class of structural or qualitative characteristics such as those characteristics, other than numbers of elements, that easily distinguish the architectures in descriptions involving diagrams (i.e., architectures that differ in qualitative characteristics *look* different on paper).

It is desired to lump the two classes of characteristics together and to treat both quantitatively, which allows the application of statistical analysis and optimization techniques.

Once the structure of a design is fixed, it is a fairly straightforward task to optimize the quantitative parameters (such as number of processing elements and amount of memory), using, for example, queuing methods. Analysis methods do not generally exist for treating a qualitative parameter as taking on values for a continuum and choosing between "values" such as a ring or a tree interconnection, or something "in between."

This research considers the following parameters.

(1) Number of processing elements (PE's)

(2) Interconnection network

(3) Speeds of the interconnection media

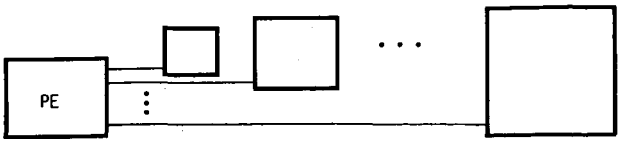

Figure 24.—Generalized model of memory hierarchy.

(4) Memory hierarchy structure (Fig. 24 gives a generalized model of memory hierarchy, as viewed from a processing element.)

(5) Size of each memory unit

(6) I/O overlap (present or not)

Programs from different classes of applications are optimally (or near-optimally) mapped to models of architectures representing a variety of parameter levels. Performance data are collected during simulation and equations relating performance to parameter levels are developed using regression analysis.

This analysis technique may be used to evaluate existing architectural designs to be used with multiple applications and for the automatic synthesis of new architectural designs.

Researchers: H.F. Standley (Univ. of Toledo) and L.J. Kiraly (NASA Lewis).

Transputer Test Bed Program

We need to develop more detailed understanding of the complex dynamic interactions that occur within increasingly sophisticated propulsion systems. Lighter weights and higher operating speeds and temperatures require system level design solutions that consider previous second-order effects. The resulting requirement for increased computing capability cannot be met by simply speeding up single processor machines. Parallel computational methods will be needed for future systems.

The transputer test bed system was conceived for parallel structures analysis methods research. The system is designed to be electronically reconfigured into a variety of different equivalent architectures so that the interplay between algorithms and architectures can be fully explored. The system is built with high-performance processors, but it is not expected to perform as well as a dedicated-function computer could.

The transputer chip is a self-contained high-performance computer. Separate processors within the transputer chip perform normal computations, manage memory, perform floating-point arithmetic functions, and manage communications with other transputers concurrently. Many transputers can be linked together to form a parallel-processing computer network by simply connecting serial communication links between transputers. Since transputers were conceived to be interconnected in large parallel arrays, the base instruction set was designed to implement a general purpose parallel-programming language called OCCAM.

The test bed program was formed by collecting independent activities from different sponsors, each of which had transputer computing in common. The program has grown from initial funding from the Director's Discretionary Fund (NASA Lewis) and now includes a phase-I Small Business Innovative Research Program contractor as well as Institute for Computational Mechanics in Propulsion (ICOMP) sponsored research.

The program is designed to develop and assess fundamentally new approaches for structures analysis which best exploit emerging parallel computing methods. There are three principal thrusts:

(1) Algorithms that absolutely require parallel computing, such as real-time digital signal processing from rotating equipment, actively controlled self-adaptive magnetic bearings, robotic trajectory optimization, and parametric gradient search methods for massive nonlinear optimization

(2) Algorithms that offer greatly improved performance such as structural multigridding analyses, parallel finite element analyses, time-domain finite elements and direct integration methods, parallel eigenvalue extraction, and structure animation

(3) Software tools to assist in parallel code development such as both fine and coarse grain data flow code analyses, a FORTRAN to OCCAM code translator, best assignments of data flow graphs to arbitrary processor networks, and determinations of optimal processor interconnection networks for given algorithms

---

Researchers: L.J. Kiraly (NASA Lewis), G.K. Ellis and F.A. Akl (ICOMP), D.C. Janetzke (NASA Lewis), A.F. Kascak (AVSCOM), E.H. Meyn and J.D. Guptill (NASA Lewis), H.F. Standley (Univ. of Toledo), and A. Wadha (Sverdrup).

Transputer-Based Finite Element Solver

This study focused on the feasibility of implementing finite element method (FEM) models on a transputer array.

Finite element programs designed to take advantage of the parallel processing environment of a transputer system were developed and implemented on a transputer system consisting of 13 transputers arranged in a singly reentrant grid (fig. 25). The performance of the transputer-based finite element solver was compared to sequential solvers on a VAX 11/780 computer and an Apollo DN660 computer. For a finite element model with 242 degrees of freedom, the solution time on the transputer system was 2.7 times faster than the VAX and 11.5 times faster than the Apollo.

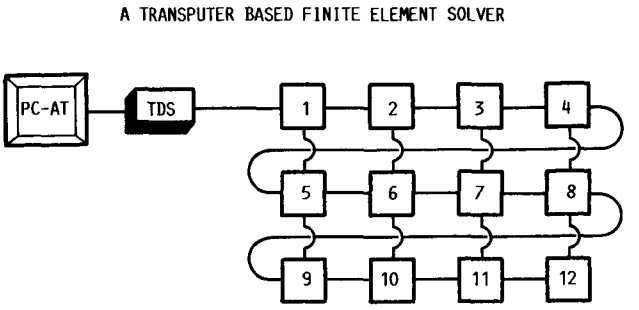

Figure 25.—Transputer network configuration. TDS is a T414 transputer on an INMOS B004 board (2 Mbytes of RAM); 1 to 12 are T414 transputers on CSA part-1 boards (256 Kbytes of RAM per transputer).

The improvement in execution time achieved with the small transputer network used in this study is significant because it can be readily expanded to much higher performance levels. Furthermore, this improvement was achieved at a cost of $15,000 for the complete system. By comparison, the Apollo system and the VAX system were, respectively, 6 and 16 times more expensive. As transputer production reaches planned volume, projected price reductions will further amplify these differences by a factor of 2 to 3. Consequently, a transputer-based finite element engine could be built that would dramatically reduce cost and time barriers for demanding finite element applications.

Innovations in network communications were instrumental to the implementation of the finite element solver. Specific communications issues resolved included broadcast and point-to-point communications. Continuing research in the related areas of hardware configuration and communication software, which minimize communication path lengths, indicates additional performance gains are possible.

Developmental work on alternative solution methods with attributes suited to parallel processing complemented the finite element solver implementation. The frontal solution method was identified as promising for adaptation to a parallel-processing environment. Beneficial attributes of this approach include concurrent stiffness matrix calculations and reduction at the element level, concurrent execution of multiple fronts, and reduced memory requirements.

This study has demonstrated that it is feasible to implement the finite element method on a transputer network. In addition, reasonable projections of the results indicate that a modular, expandable finite element analysis tool of extraordinary capability could be assembled (table II and fig. 26).

TABLE II.—PROJECTED SOLUTION TIMES FOR LARGE PROBLEMS

Degrees of freedom	Solution times				
	Apollo DN660	Transputer development system (TDS)—single T414 transputers	VAX 11/780 with floating point accelerator	TDS + 12 transputers (all T414s)	Workstation with 40 T800 transputers
500	1 hr, 3 min	57 min	31 min	9 min	15 sec
750	3 hr, 20 min	3 hr	1 hr, 45 min	27 min	48 sec
1 000	7 hr, 45 min	6 hr, 45 min	4 hr, 12 min	1 hr	1 min, 50 sec
2 000	60 hr	51 hr	34 hr	7 hr, 45 min	14 min
5 000	38 days	32 days	22 days	4 days, 22 hr	3 hr, 30 min
10 000	302 days	250 days	184 days	39 days	1 day, 4 hr

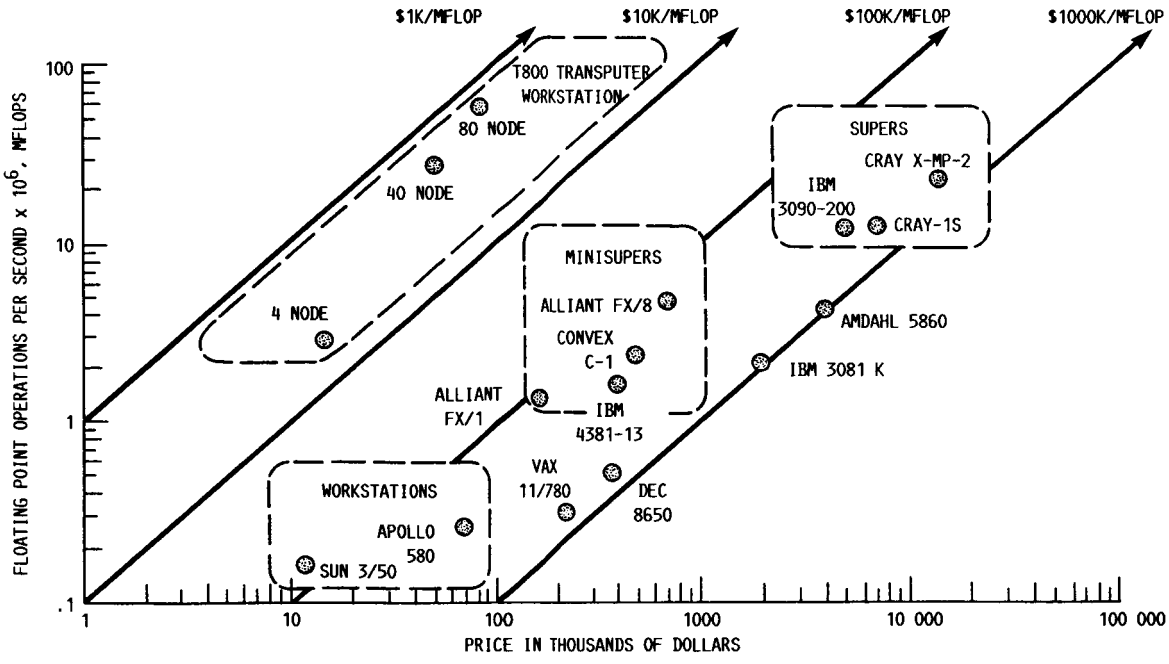

Figure 26.—Performance and price comparisons for transputers and other computing systems.

Researchers: L.J. Kiraly (NASA Lewis) and J. Watson (Sparta).

Robots for Manipulation in a Microgravity Environment

There are two related control problems associated with the operation of robots in a microgravity environment. The first is the transportation of specimens without exceeding microgravity accelerations on the specimens themselves. The second control problem is associated with the operation of the robot without transmission of reactions to the surrounding environment. For every motion of the manipulator, there will be a counteracting reaction at the manipulator base. These reactions may be transmitted to the space station where they will disturb the microgravity environment.

The simplest solution for eliminating, or reducing, the base reactions is to move the robot arm slowly so that forces are maintained below acceptable levels. For situations that permit high accelerations at the end-effector, such as the transportation of nonsensitive test equipment or supplies, swifter motions may be desirable. Under this condition, devices or control strategies that compensate for the resulting momentum must be employed. If the robot is free-floating, then similar strategies could be used so that the motion of the base does not obstruct, or collide with, other activities.

This research is concerned with the development of techniques for minimizing the robot base reaction so

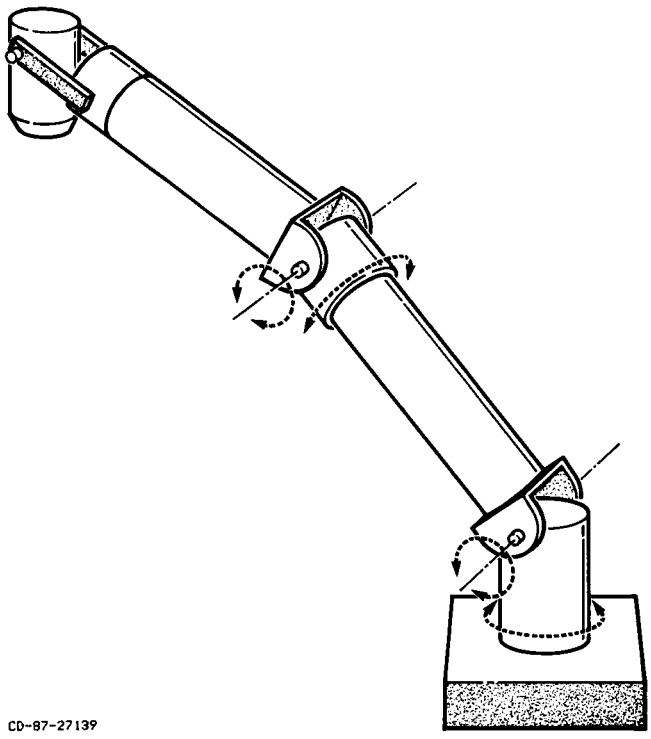

Figure 27.—Conceptual design of traction-driven manipulator with two-degree-of-freedom joints.

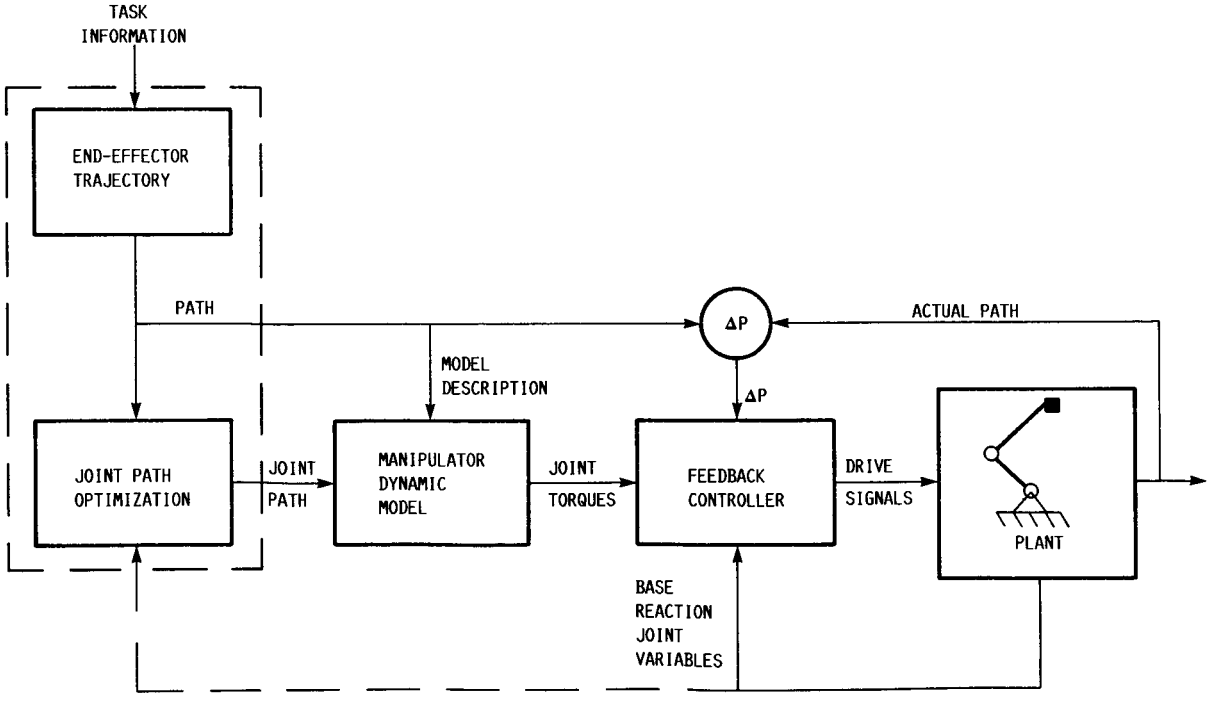

Figure 28.—Control strategy for redundant joint manipulator.

as not to disturb the microgravity environment. Three approaches are discussed for achieving this goal. The first and most straightforward method of momentum compensation is to attach actuators at the robot base which supply counteracting forces and moments that cancel the reactions resulting from the motions of the manipulators. These actuators can take the form of mechanisms such as thrusters, control-moment gyros, or proof-mass actuators. This approach is advantageous because it is relatively simple to design and implement, but it has disadvantages in that it adds mass to the robot without any increase in motion flexibility (although, mobility of the base is possible with thrusters).

Another approach for momentum compensation is to include more joints, or degrees of freedom, in the manipulator than are required to accomplish the specified motion of the end-effector. This can be achieved by incorporating extra joints in the robot arm. With redundant degrees of freedom there are an infinite number of possible motions of the joints that will satisfy a specified end-effector trajectory. By utilizing an appropriate optimization strategy, the combination of joint motions that minimizes the base reactions can be determined (figs. 27 and 28).

The final approach discussed in this paper for momentum compensation is the utilization of a redundant (or counterbalance) arm sharing a common base with the worker arm. The redundant arm task is to produce equal, and opposite, base reactions of the worker arm which nullify the net base reactions. When momentum compensation is not necessary, the redundant arm can work with the other arm, increasing task adaptability. The redundant arm could be constructed as a duplicate, or a scaled down version, of the worker arm.

Researchers: R.D. Quinn (Case Western Reserve Univ.) and C. Lawrence (NASA Lewis).

Trajectory Design for Robotic Manipulators in Space Applications

Robotic manipulators used in space applications are expected to operate under microgravity conditions. Base reactions of a space manipulator are directly exerted on the supporting space structure which would be typically a space vehicle (e.g., a space shuttle) or a space station. It is desirable to make these reactions as small as possible in order to reduce their influence on the dynamics of the supporting space structure. This will help control the space structure, which is a crucial consideration in its own right in space applications. Furthermore, in delicate experiments conducted in space, the test specimen would have to be moved carefully without subjecting it to excessive accelerations and jerks, but at reasonably high speeds. It follows that minimization of base reactions and limitation of end-effector accelerations and jerks are important performance objectives for space manipulators.

This research developed a trajectory generation method for space manipulators. The approach employed a manipulator with redundant kinematics. The method was implemented in two steps. First, the end-effector trajectory was developed to satisfy the acceleration and jerk limitations. Next, the joint trajectories were developed to minimize a quadratic cost function in base forces and base moments. Kinematic redundancy of the manipulator is employed here.

A three-revolute manipulator executing planar motions was considered as an example. The end-effector trajectory was divided into equal time steps. During the first step, an exhaustive search method was used to determine the initial configuration as well as the initial parameters that will minimize the cost function. Then, unconstrained optimization was carried out for the subsequent steps to determine the optimal trajectory.

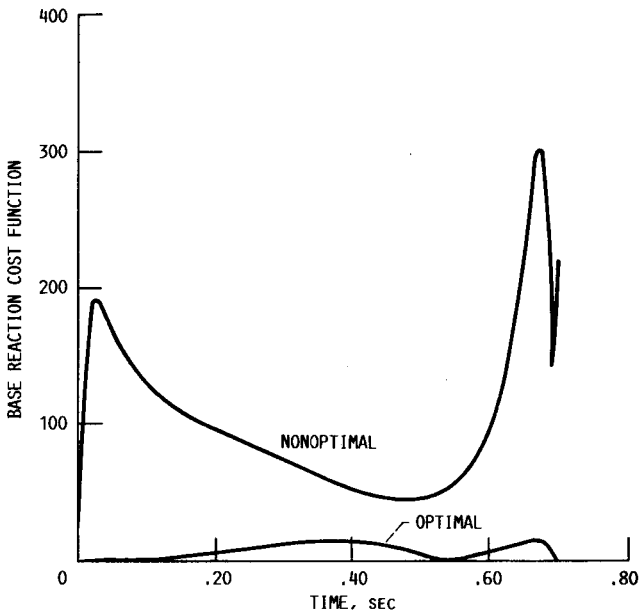

Figure 29.—Optimal and nonoptimal cost functions for space manipulator trajectory design.

Figure 29 shows the resulting optimal and nonoptimal base reactor cost functions. The relative magnitude of the optimal curve is consistently close to zero in comparison to that of the nonoptimal curve. This indicates that the ideal objective of zero reactions would be within reach. The results show a great promise for utilizing kinematic redundancy in minimizing base reactions.

Researchers: C.W. deSilva and C.L. Chung (Carnegie-Mellon Univ.) and C. Lawrence (NASA Lewis).

Development of a Dynamic High-Temperature Flexible Variable-Geometry Engine Seal

Variable-geometry engine panel-sidewall seals are required to seal highly pressurized (up to 100 psi) engine cavities, operate at temperatures in excess of 2000 °F, and conform "serpentine" style to sidewall deformations that can be as much as 0.25 in. Because of high-temperature strength limitations, current state-of-the-art metal seals typical of exhaust nozzle seals generally operate to pressures and temperatures less than 50 psi and 1500 °F, respectively, and only conform to gap openings less than 0.150 in. The seal concept recently developed shows promise in meeting the extreme seal demands because of its flexible structure and high-temperature material components.

The seal consists of multiple layers of concentric braided ceramic sleeves internally filled with small ceramic balls providing a highly flexible, minimally porous seal for gaps between moving and stationary engine panels (fig. 30). The ceramic sleeves are made from commercially available aluminoboriasilicate material, which maintains strength and flexibility up to 2500 °F and has successfully flown as a flexible

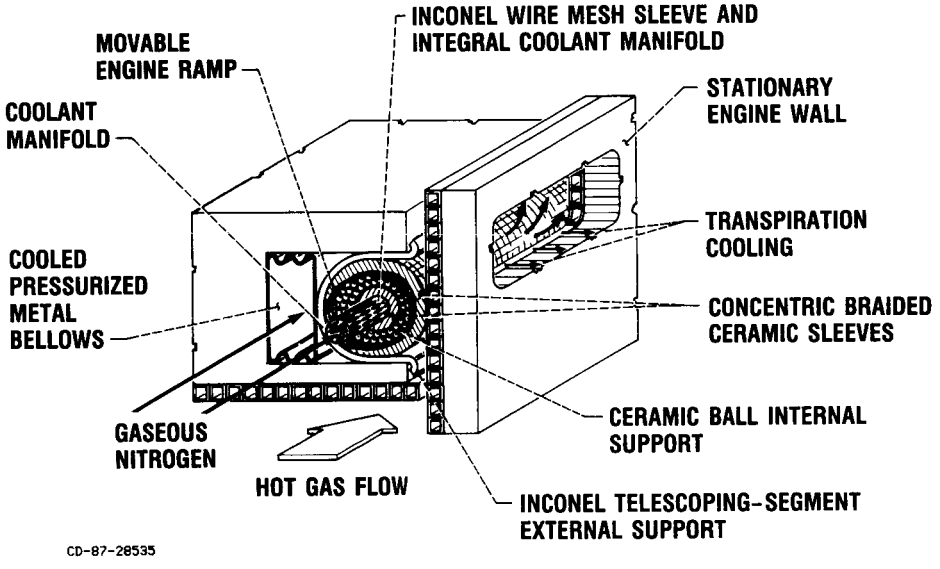

Figure 30.—Dynamic, high-temperature flexible seal.

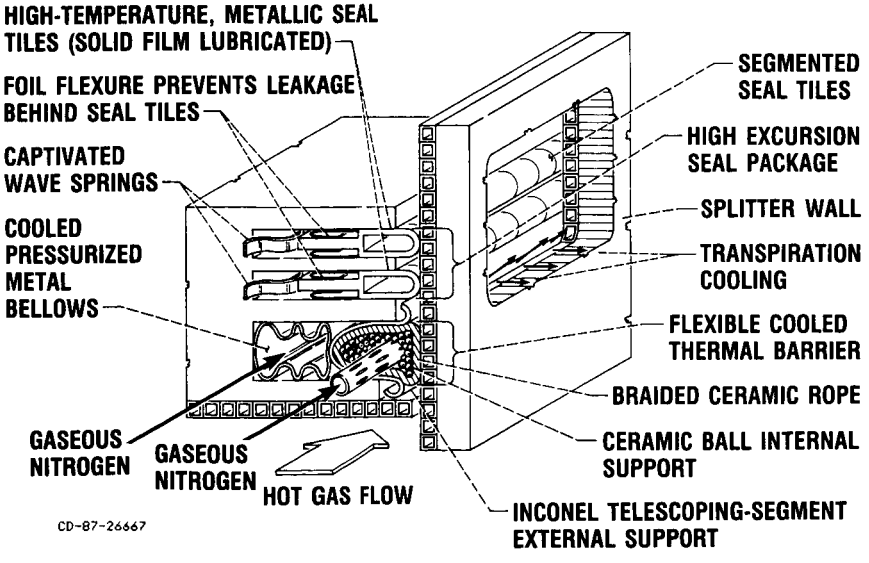

Figure 31.—Two-stage, high-temperature flexible seal.

thermal barrier on the space shuttle. Ceramic balls (made of Al_2O_3 or ZrO, etc.) minimize the relatively high porosity of the ceramic sleeves and provide a further insulator for the internal spring support. The innermost sleeve made of an Inconel wire mesh provides seal springback (i.e., memory) and preload capabilities.

For engine applications where temperatures exceed the capability of the materials, a transpiration cooling feature (as shown in fig. 30) can be integrated into the design inside the Inconel wire mesh. Coolant (such as gaseous nitrogen) flows down the center coolant manifold evenly distributing coolant axially along the seal venting radially outward through the various layers providing very effective transpiration cooling for the system.

At critical engine areas where near absolute sealing is required, the seal may be combined with a variety of other seal concepts such as that shown in figure 31. In this arrangement the seal is used as the first stage to provide a thermal barrier and initial seal capability. The second seal stage operating in the relatively cooler (1500 °F) environment is designed to provide final sealing capability. The second stage consists of two layers of high-temperature segmented seal tiles sprung outward against the engine splitter wall with wavesprings. The traveling foil flexures prevent leakage behind the seal tiles. Because of the moving parts a high-temperature solid film lubricant would be required to ensure smooth operation.

Researchers: B. Steinetz (NASA Lewis) and P.J. Sirocky (Sverdrup).

Appendix—Researchers

Akl, F.A. . . . . Institute for Computational Mechanics in Propulsion (ICOMP), NASA Lewis Research Center, Cleveland, Ohio

Brown, G.V. . . . . NASA Lewis Research Center, Cleveland, Ohio

Chung, C.L. . . . . Carnegie-Mellon University, Pittsburgh, Pennsylvania

deSilva, C.W. . . . . Carnegie-Mellon University, Pittsburgh, Pennsylvania

Ellis, G.K. . . . . Institute for Computational Mechanics in Propulsion (ICOMP), NASA Lewis Research Center, Cleveland, Ohio

Ernst, M.A. . . . . NASA Lewis Research Center, Cleveland, Ohio

Fleming, D.P. . . . . NASA Lewis Research Center, Cleveland, Ohio

Guptill, J.D. . . . . NASA Lewis Research Center, Cleveland, Ohio

Huckelbridge, A.A. . . Case Western Reserve University, Cleveland, Ohio

Janetzke, D.C. . . . . NASA Lewis Research Center, Cleveland, Ohio

Kascak, A.F. . . . . U.S. Army Aviation Research and Technology Activity—AVSCOM, NASA Lewis Research Center, Cleveland, Ohio

Kaza, K.R.V. . . . . NASA Lewis Research Center, Cleveland, Ohio

Kielb, R.E. . . . . NASA Lewis Research Center, Cleveland, Ohio

Kiraly, L.J. . . . . NASA Lewis Research Center, Cleveland, Ohio

Lawrence, C. . . . . NASA Lewis Research Center, Cleveland, Ohio

Lin, R. . . . . Texas A&M University, College Station, Texas

Mehmed, O. . . . . NASA Lewis Research Center, Cleveland, Ohio

Meyn, E.H. . . . . NASA Lewis Research Center, Cleveland, Ohio

Montague, G.T. . . . . Sverdrup Technology, Inc. (Lewis Research Center Group), NASA Lewis Research Center, Cleveland, Ohio

Moss, L.A. . . . . Sverdrup Technology, Inc. (Lewis Research Center Group), NASA Lewis Research Center, Cleveland, Ohio

Murthy, D.V. . . . . The University of Toledo, Resident Research Associate at NASA Lewis Research Center, Cleveland, Ohio

Narayanan, G.V. . . . . Sverdrup Technology, Inc. (Lewis Research Center Group), NASA Lewis Research Center, Cleveland, Ohio

North, C.M. . . . . Rose-Hulman Institute of Technology, Terre Haute, Indiana

Palazzolo, A.B. . . . . Texas A&M University, College Station, Texas

Quinn, R.D. . . . . Case Western Reserve University, Cleveland, Ohio

Ropchock, J.J. . . . . NASA Lewis Research Center, Cleveland, Ohio

Sankar, L.N. . . . . Georgia Institute of Technology, Atlanta, Georgia

Sirocky, P.J. . . . . Sverdrup Technology, Inc. (Lewis Research Center Group), NASA Lewis Research Center, Cleveland, Ohio

Smith, T.E. . . . . Sverdrup Technology, Inc. (Lewis Research Center Group), NASA Lewis Research Center, Cleveland, Ohio

Smolinski, P. . . . . University of Pittsburgh, Pittsburgh, Pennsylvania

Standley, H.M. . . . . The University of Toledo, Toledo, Ohio

Steinetz, B. . . . . NASA Lewis Research Center, Cleveland, Ohio

Wadha, A. . . . . Sverdrup Technology, Inc. (Lewis Research Center Group), NASA Lewis Research Center, Cleveland, Ohio

Watson, J. . . . . Sparta, Inc., Huntsville, Alabama

Williams, M. . . . . Purdue University, West Lafayette, Indiana

Wu, J. . . . . Georgia Institute of Technology, Atlanta, Georgia

Bibliography

Brown, G.V.; and North, C.M.: The Impact Damped Harmonic Oscillator in Free Decay. NASA TM–89897, 1987.

Cameron, T.M., et al.: An Integrated Approach for Friction Damper Design. The Role of Damping in Vibration and Noise Control, L. Rogers and J.C. Simonis, eds., ASME, 1987, pp. 205–212.

Chen, S.H.; and Williams, M.H.: A Panel Method for Counter Rotating Propfans. AIAA Paper 87–1890, June 1987.

Ernst, M.A.; and Lawrence, C.: Hub Flexibility Effects on Propfan Vibrations. NASA TM–89900, 1987.

Favenesi, J.; Daniel, A.; and Bower, M.: Transputer Based Finite Element Solver, Phase I, SBIR. Sparta Inc., Huntsville, AL, (NASA Contract NAS3–25126) July 1987.

Gallardo, V.C.; and Black, G.: Blade Loss Transient Dynamic Analysis. Vol. I, Task II—TETRA 2 Theoretical Development. NASA CR–179632, 1986.

Hoffman, J.A.; and Sridhar, S.: WEST–3 Wind Turbine Simulator Development, Vol. 3: Software. (PPI–FID–300086–VOL–3, Paragon Pacific Inc.; NASA Contract DEN3–247) DOE/NASA–0247/3, NASA CR–174983, 1985.

Huckelbridge, A.A.; and Lawrence, C.: Identification of Structural Interface Characteristics Using Component Mode Synthesis. Modal Testing and Analysis, T.G. Carne and J.C. Simonis, eds., ASME, 1987. (NASA TM–88960).

Kaza, K.R.V., et al.: Analytical Flutter Investigation of a Composite Propfan Model. 28th Structures, Structural Dynamics and Materials Conference, Part 2A, AIAA, 1987, pp. 84–97. (NASA TM–88944).

Kaza, K.R.V., et al.: Analytical and Experimental Investigation of Mistuning in Propfan Flutter. 28th Structures, Structural Dynamics and Materials Conference, Part 2A, AIAA, 1987, pp. 98–110. (NASA TM–88959).

Kennedy, F.E.: Thermomechanical Effects in High-Speed Seal Rubs. NASA CR–180418, 1987.

Kielb, R.E.; and Crawley, E.F.: Bladed Disk-Assemblies. ASME, 1987.

Kiraly, L.J.: Structural Dynamic Measurement Practices for Turbomachinery at the NASA Lewis Research Center. NASA TM–88857, 1986.

Lawrence, C., et al.: A NASTRAN Primer for the Analysis of Rotating Flexible Blades. NASA TM–89861, 1987.

McGee, O.G.: Finite Element Analysis of Flexible, Rotating Blades. NASA TM–89906, 1987.

Moss, L.A.; and Smith, T.E.: SSME Single Crystal Turbine Blade Dynamics. NASA CR–179644, 1987.

Murthy, D.V.; and Haftka, R.T.: Approximations to Eigenvalues of Modified General Matrices. 28th Structures, Structural Dynamics and Materials Conference, Part 2B, AIAA, 1987, pp. 1032–1045.

Murthy, D.V.; and Kaza, K.R.V.: A Computational Procedure for Automated Flutter Analysis. NASA TM–100171, 1987.

Pope, A.N.; and Pugh, D.W.: Development of Gas-to-Gas Lift Pad Dynamic Seals. (R87–AEB432, General Electric Co.; NASA Contract NAS3–20043) NASA CR–179486, 1987.

Posta, S.J.; and Brown, G.V.: A Low-Cost Optical Data Acquisition System for Vibration Measurement. NASA TM–88907, 1986.

Quinn, R.D.; and Lawrence, C.: Robots for Manipulation in a Micro-Gravity Environment. Proceedings of Sixth VPI and SU/AIAA Symposium on Dynamics and Control of Large Structures, Virginia Polytechnic Institute, June 1987.

Ramsey, J.K.; and Kaza, K.R.V.: Concentrated Mass Effects on the Flutter of a Composite Advanced Turboprop Model. NASA TM–88854, 1986.

Reddy, T.S.R.; and Kaza, K.R.V.: A Comparative Study of Some Dynamic Stall Models. NASA TM–88917, 1987.

Smith, A.F.; and Brooks, B.M.: Dynamic Response of Two Composite Propfan Models on a Nacelle/Wing/Fuselage Half Model. (HSER–11058, Hamilton Standard; NASA Contract NAS3–24088) NASA CR–179589, 1986.

Smith, A.F.; and Brooks, B.M.: Dynamic Response and Stability of a Composite Propfan Model. (HSER–11057, Hamilton Standard; NASA Contract NAS3–24088) NASA CR–179528, 1986.

Sridhar, S.: WEST–3 Wind Turbine Simulator Development, Vol. 1: Summary. (PPI–FID–300101–VOL–1, Paragon Pacific Inc.; NASA Contract DEN3–247) DOE/NASA–0247/1–VOL–1, NASA CR–174981, 1986.

Sridhar, S.: WEST–3 Wind Turbine Simulator Development, Vol. 2: Verification. (PPI–FID–300102–VOL–2, Paragon Pacific Inc.; NASA Contract DEN3–247) DOE/NASA–0247/2, NASA CR–174982, 1985.

Standley, H.M.: A Very High Level Language for Large-Grained Data Flow. 1987 ACM Fifteenth Annual Computer Science Conference, Association for Computing Machinery, 1987, pp. 191–195.

Subrahmanyam, K.B.; and Kaza, K.R.V.: Non-Linear Flap-Lag-Extensional Vibrations of Rotating, Pretwisted, Preconed Beams Including Coriolis Effects. Int. J. Mech. Sci., vol. 29, no. 1, 1987, pp. 29–43.

Subrahmanyam, K.B., et al.: Nonlinear Vibration and Stability of Rotating, Pretwisted, Preconed Blades Including Coriolis Effects. J. Aircraft, vol. 24, no. 5, May 1987, pp. 342–352.

Subrahmanyam, K.B.; and Kaza, K.R.V.: Influence of Third-Degree Geometric Nonlinearities on the Vibration and Stability of Pretwisted, Preconed, Rotating Blades. Eighth International Symposium on the Breathing Engines, F.S. Billig, ed., AIAA, 1987, pp. 465–479.

Turnberg, J.E.: Unstalled Flutter Stability Predictions and Comparisons to Test Data for a Composite Propfan Model. (HSER–11056, Hamilton Standard: NASA Contract NAS3–24088) NASA CR–179512, 1986.

Wu, J.C.; Kaza, K.R.V.; and Sankar, L.N.: A Technique for the Prediction of Airfoil Flutter Characteristics in Separated Flow. 28th Structures, Structural Dynamics and Materials Conference, Part 2B, AIAA, 1987, pp. 664–673.

NASA
National Aeronautics and Space Administration

Report Documentation Page

1. Report No.	2. Government Accession No.	3. Recipient's Catalog No.
NASA TM–100279		

4. Title and Subtitle	5. Report Date
Structural Dynamics Branch Research and Accomplishments for FY 1987	May 1988
	6. Performing Organization Code
7. Author(s)	8. Performing Organization Report No.
	E–3920
	10. Work Unit No.
	505–63–1B
9. Performing Organization Name and Address	11. Contract or Grant No.
National Aeronautics and Space Administration Lewis Research Center Cleveland, Ohio 44135–3191	
	13. Type of Report and Period Covered
	Technical Memorandum
12. Sponsoring Agency Name and Address	14. Sponsoring Agency Code
National Aeronautics and Space Administration Washington, D.C. 20546–0001	

15. Supplementary Notes

16. Abstract

This publication contains a collection of fiscal year 1987 research highlights from the Structural Dynamics Branch at NASA Lewis Research Center. Highlights from the branch's four major work areas—Aeroelasticity, Vibration Control, Dynamic Systems, and Computational Structural Methods—are included in the report as well as a complete listing of the FY 87 branch publications.

17. Key Words (Suggested by Author(s))	18. Distribution Statement
Aeroelasticity Vibration control Robotics Computational structural methods	Unclassified—Unlimited Subject Category 39

19. Security Classif. (of this report)	20. Security Classif. (of this page)	21. No of pages	22. Price*
Unclassified	Unclassified	36	A03

*For sale by the National Technical Information Service, Springfield, Virginia 22161